

Hypoplastic Modelling of Pre-Failure Behaviour of Sand Against Experimental Data

Krzysztof Głębowicz

Institute of Hydro-Engineering, Polish Academy of Sciences,
ul. Kościarska 7, 80-328 Gdańsk, Poland, e-mail: dexter@ibwpan.gda.pl

(Received February 10, 2005; revised January 04, 2006)

Abstract

The aim of this article is to compare experimentally determined strains of sand with theoretical calculations made on the base of the theory of hypoplasticity. During the study ‘Skarpa’ sand was examined in the triaxial apparatus with local measurement of vertical and lateral strains. Results obtained were used to calibrate 8-parameter von Wolffersdorff model. Subsequently, the behaviour of loose and dense sandy samples subjected to different stress paths was predicted.

Key words: hypoplasticity, constitutive equation, sand, deformation, anisotropy

1. Introduction

The theory of hypoplasticity (Kolymbas 1985) is an alternative to the elasto-plasticity method of modelling deformations of granular materials. The main feature of this theory is that only one tensorial equation is needed to calculate both reversible and irreversible deformations of sand.

The aim of the following article is to analyse the capability of hypoplastic equation to reproduce the deformations of the soil subjected to various stress paths in triaxial conditions, in the pre-failure range of deformations (up to a few per cent of axial strain). This issue is essential for a proper predictions of settlement of the foundations.

In this publication, von Wolffersdorff’s hypoplastic equation was used in the analysis of deformations of ‘Skarpa’ sand, the behaviour of which was examined mostly in a modern triaxial apparatus. The calibration of the model was carried out based on the results of simple geotechnical tests. Subsequently, the behaviour of loose and dense sandy samples subjected to various stress paths (e.g. isotropic compression and extension path, pure shearing stress paths) was predicted.

2. Experimental Programme

‘Skarpa’ sand, the characteristics of which are presented in Table 1, was examined in the modern, computer-controlled triaxial apparatus from GDS Instruments Ltd., which comprises the classic Bishop & Wesley-type triaxial cell with both 38 mm and 50 mm diameter pedestals and top caps, one internal submersible 5 kN load cell, three standard pressure/volume controllers configured with volume change measurement and a 16 bit data acquisition device for accurate measurement of all transducers, RS232 computer interface and controlling software. Additionally, triaxial apparatus has been equipped with 3 gauges for local measurement of both vertical and horizontal deformations, which comprise two parts, independently connected to the sample, in the way presented in Fig. 1a. The upper part of the gauge is built of a metal arm, holding the magnet cluster, while the lower one is a semiconductor placed on a pad. The parts are able to move independently due to the deformations of the sample. Measurements of deformations are based on Hall effect, schematically presented in Fig. 1b, which involves a relative movement of magnet and semiconductor changing the magnetic field, penetrating the semiconductor. The resulting Hall voltage V_H changes were recorded by the data acquisition system and allowed to calculate the value of deformations. Each base of vertical deformation gauge was mounted to the sample 20 mm from its upper and lower end in order to eliminate bedding errors. The practical resolution of the gauges for a sample with an average diameter was 10^{-4} , thus local measurement method is more precise and gives more reliable results than any indirect method.

Table 1. Basic characteristics of ‘Skarpa’ sand

Mean diameter	D_{50}	0.42 mm
Minimum void ratio	e_{\min}	0.432
Maximum void ratio	e_{\max}	0.677
Coefficient of uniformity	C_u	2.5
Specific gravity	G	2.65
Minimum int. friction angle	φ	33°
Maximum int. friction angle	φ_{\max}	41°

Moreover, a number of experiments was carried out in an oedometer with ability to measure lateral stresses. Used equipment has been described in details in a number of publications (see, for example, Sawicki, Świdziński 1995, Świdziński, Mierczyński 2002).

The aim of experimental research was to examine deformations of ‘Skarpa’ sand in two states – loose and dense, subjected to some chosen simple stress paths in triaxial conditions. The Authors of the research programme preferred to collect wide set of data concerning one sand instead of small data sets concerning a large number of materials (Sawicki, Świdziński 2002, Sawicki, Chybicki 2003). Initial density state of examined samples was either loose ($I_D < 0.3$) or dense ($I_D > 0.7$), where I_D stands for index of density:

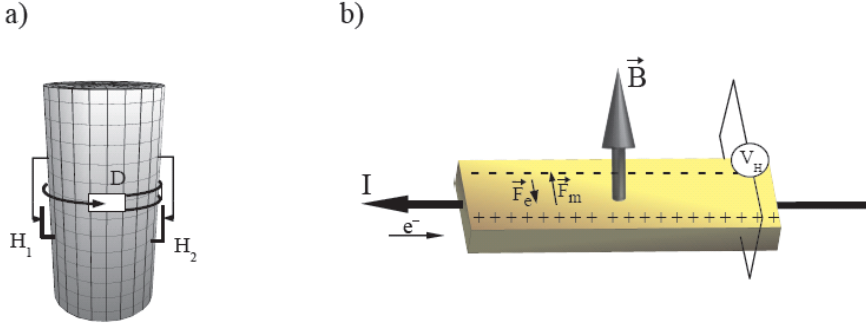


Fig. 1. a) arrangement of deformation gauges on the sand sample. H_1 and H_2 – vertical deformation gauges, D – radial deformation gauge; b) schematic drawing of Hall effect where \vec{B} is the magnetic field, I – direction of the electric current, \vec{F}_e – electric force from charge build-up, \vec{F}_m – magnetic force on negative charge carriers, V_H – Hall voltage

$$I_D = \frac{e_{\max} - e}{e_{\max} - e_{\min}}. \quad (1)$$

Each experiment was repeated at least once to avoid possibility of mistakes and provide some simple statistics, since it is impossible to prepare identical samples from different sets of grains. Consequently, a deviation of strains level is expected in similar experiments.

The catalogue of collected experimental data contains unique information, which can be helpful for verification of existing soil models (e.g. Sawicki 2003) or can serve as a basis to create and calibrate new soil models.

Exemplary results of experiments will be presented in the further part of the article.

In the paper all experimental and theoretical data are presented in traditional convention, where the compression denotes positive volumetric changes. Relations between stresses and strains are presented in the space of stress and strain invariants, defined as follows:

$$p = \frac{\sigma_1 + 2\sigma_3}{3}, \quad (\text{mean stress}), \quad (2)$$

$$q = \sigma_1 - \sigma_3, \quad (\text{deviatoric stress}), \quad (3)$$

$$\varepsilon_v = \varepsilon_1 + 2\varepsilon_3, \quad (\text{volumetric strain}), \quad (4)$$

$$\varepsilon_q = \frac{2}{3}(\varepsilon_1 - \varepsilon_3), \quad (\text{deviatoric strain}), \quad (5)$$

where: σ_1 – vertical stress, σ_3 – horizontal stress, ε_1 – vertical strain and ε_3 is horizontal strain. Standard stress unit in this publication is 10^5 Pa and strain unit is 10^{-3} . For example, expression $p = 5$ states that the value of the mean stress equals 0.5 MPa, and $\varepsilon_v = 3$ means that the value of volumetric strain amounts to 3×10^{-3} .

3. Calibration of von Wolffersdorff Model

The modified version of von Wolffersdorff's equation (von Wolffersdorff 1996), which fulfils the Matsuoka and Nakai yield condition (Matsuoka, Nakai 1977), takes the following form:

$$\overset{\circ}{\mathbf{T}} = f_b f_e \frac{1}{tr \hat{\mathbf{T}}^2} \left[F^2 \mathbf{D} + a^2 \hat{\mathbf{T}} tr(\hat{\mathbf{T}} \mathbf{D}) + f_d a F (\hat{\mathbf{T}} + \hat{\mathbf{T}}^*) \sqrt{tr \mathbf{D}^2} \right], \quad \hat{\mathbf{T}} = \frac{\mathbf{T}}{tr \mathbf{T}} \quad (6)$$

where

$$\mathbf{T}^* = \mathbf{T} - \frac{1}{3} (tr \mathbf{T}) \mathbf{I} \quad (7)$$

is the deviatoric stress. By reduction of the tensorial equation (6) to the triaxial case with axial symmetry ($T_2 = T_3$), it is possible to present this equation in the form of a system of two differential equations:

$$\begin{aligned} \dot{T}_1 &= f_b f_e \frac{(T_1 + 2T_2)^2}{T_1^2 + 2T_2^2} \times \\ &\times \left[F^2 D_1 + a^2 \frac{T_1 D_1 + 2T_2 D_2}{(T_1 + 2T_2)^2} T_1 + f_d \frac{a}{3} F \frac{5T_1 - 2T_2}{T_1 + 2T_2} \sqrt{D_1^2 + 2D_2^2} \right], \\ \dot{T}_2 &= f_b f_e \frac{(T_1 + 2T_2)^2}{T_1^2 + 2T_2^2} \times \\ &\times \left[F^2 D_2 + a^2 \frac{T_1 D_1 + 2T_2 D_2}{(T_1 + 2T_2)^2} T_2 + f_d \frac{a}{3} F \frac{4T_1 - T_2}{T_1 + 2T_2} \sqrt{D_1^2 + 2D_2^2} \right]. \end{aligned} \quad (8)$$

Introducing the following functions, equation (6) depends only on parameters, which can be estimated on the basis of standard mechanical parameters of sand and simple geotechnical tests (Bauer 1996, Gudehus 1996, Herle, Gudehus 1999).

$$a = \frac{\sqrt{3} (3 - \sin \varphi)}{2\sqrt{2} \sin \varphi}, \quad (9)$$

where φ is the residual (critical) internal friction angle;

$$f_d = \left(\frac{e - e_d}{e_c - e_d} \right)^\alpha, \quad (10)$$

$$f_b = \frac{h_s}{n} \left(\frac{e_{i0}}{e_{c0}} \right)^\beta \frac{1 + e_i}{e_i} \left(\frac{3p}{h_s} \right)^{1-n} \left[3 + a^2 - a\sqrt{3} \left(\frac{e_{i0} - e_{d0}}{e_{c0} - e_{d0}} \right)^\alpha \right]^{-1}, \quad (11)$$

$$f_e = \left(\frac{e_c}{e} \right)^\beta. \quad (12)$$

Here f_d is relative void ratio (cf. Eq. 1), f_b is the barotropy coefficient (Greek word for pressure dependency), and f_c is the density factor. f_d and f_c coefficients are also called the pyknotropy factors, since pyknotropy is the Greek word for dependence on density.

$$F = \sqrt{\frac{1}{8} \tan^2 \psi + \frac{2 - \tan^2 \psi}{2 + \sqrt{2} \tan \psi \cos 3\vartheta}} - \frac{1}{2\sqrt{2}} \tan \psi \quad (13)$$

where

$$\tan \psi = \sqrt{2} \left| \frac{T_1 - T_2}{T_1 + 2T_2} \right|, \quad \cos 3\vartheta = \text{sign}(T_2 - T_1). \quad (14)$$

e_d , e_c and e_i are adequately minimal, maximal and critical void ratios, which are functions of the mean pressure according to the formula:

$$\frac{e_d}{e_{d0}} = \frac{e_c}{e_{c0}} = \frac{e_i}{e_{i0}} = \exp \left[- \left(\frac{3p}{h_s} \right)^n \right], \quad (15)$$

where e_{d0} , e_{c0} and e_{i0} are values of these parameters for $p = 0$.

Determination of parameters of von Wolffersdorff's model was proceeded in two stages. The first one was the estimation of these parameters in the way presented by Herle and Gudehus (1999). Subsequently, minimalisation procedure was applied in order to specify calibration of the model.

3.1. Friction Angle φ

Internal friction angle can be determined by conducting a series of standard triaxial compression tests in a triaxial apparatus with use of different lateral stresses. Shearing has to be carried on up to the Coulomb-Mohr envelope, which is equivalent to failure of the soil sample.

As a result of series of experiments the pairs of coordinates (σ_1, σ_3) obtained are drawn on diagram and are used in drawing the Coulomb-Mohr circles, as presented in Fig. 2. Straight line tangent to circles is tangential stiffness for shearing while the angle of its slope is the desired angle of internal friction.

In the von Wolffersdorff's model the φ parameter corresponds with residual state of soil. Experiments carried out for initially loose sand give $\varphi = 33^\circ$. During the numerical calculations it was assumed, that the angle of internal friction was obtained with acceptable precision and its value is treated as constant.

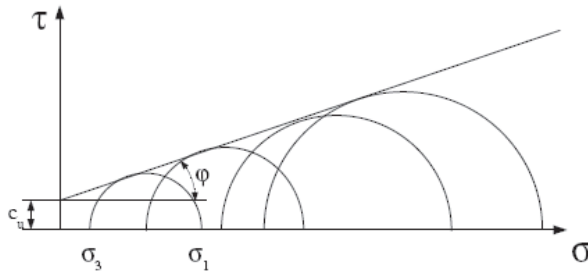


Fig. 2. Determination of the internal friction angle from triaxial compression tests in the triaxial apparatus

3.2. Void Ratio Boundary Parameters

Parameters e_d , e_c and e_i designate particular boundary functions of void ratio. These parameters are respectively: minimal, maximal and critical void ratio. Parameter e_i applies for void ratio for the loosest sand, which can exist under given stress. Above this value the skeleton of sand does not exist. Soil sample subjected to the triaxial compression test has $e = e_c$, when the Coulomb-Mohr envelope is reached. Parameter e_d is the minimal void ratio, which could be reached after cyclic shearing of the soil sample. In the von Wolffersdorff model these parameters decrease, when the mean pressure $p = \frac{\sigma_1 + \sigma_2 + \sigma_3}{3}$ increases according to equation (15), where e_{d0} , e_{c0} and e_{i0} are values of these parameters for $p = 0$. Obviously these are theoretical values, determined from extrapolation, because non-stress state can not be achieved in Earth's gravity. Relation (15) was experimentally confirmed for a wide range of mean stress in the isotropic case.

Parameters e_{d0} , e_{c0} and e_{i0} can be estimated by simple geotechnical tests. According to particular experimental results (Herle, Gudehus 1999), the following relations of e_{\min} and e_{\max} (Table 1) and hypoplastic parameters were accepted and widely used (e.g. Tejchman 2004):

$$e_{d0} \approx e_{\min}, \quad (16)$$

$$e_{c0} \approx e_{\max}, \quad (17)$$

$$e_{i0} \approx 1.2e_{\max}. \quad (18)$$

In the case of 'Skarpa' sand these relations were used as first approximation as well. However, to determine the e_{\min} value, classic Proctor test was carried out instead of cyclic shearing in the simple shearing apparatus, which would give higher maximum density of the sand. Thus, some variations of these values (especially e_{d0}) are expected in the second stage of the calibration procedure.

3.3. Granulate Hardness h_s and Exponent n (Compression Parameters)

Granulate hardness is the only parameter in the equation with dimension of stress which is referred to as reference pressure, while parameter n controls the reaction of the sample on mean pressure level.

For estimating h_s and n , a steady state line was used, determined for ‘Skarpa’ sand by Świdziński and Mierczyński (2005). Steady state line is quite a new concept, which appeared in geomechanics in recent years. This line separates contractive and dilative soils response in $(p', \lg e)$ space. A number of experiments shows, that soil under shearing in the triaxial apparatus tends to the steady state of deformation, located on this line (Fig. 3). It seems to correspond with e_c function (see Eq. 15) and it looks to be easier to calibrate h_s and n by this method, than those suggested by Herle and Gudehus (1999), which is for comparison presented in short hereafter.

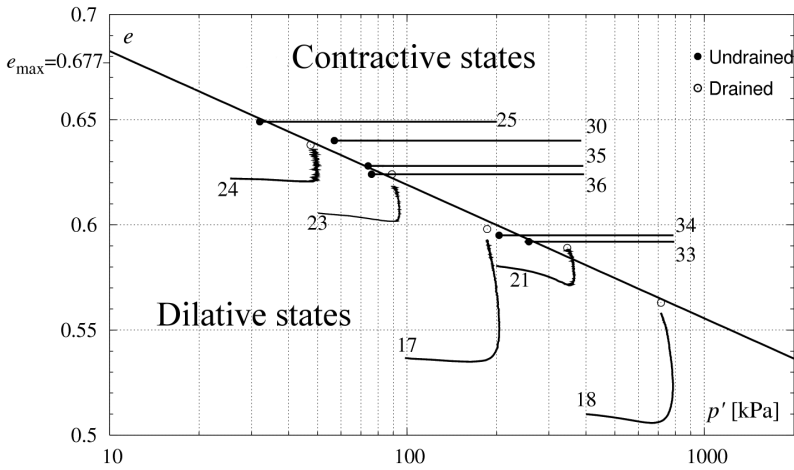


Fig. 3. Steady state line for ‘Skarpa’ sand (after Świdziński and Mierczyński (2005), Fig. 8)

For the sand examined, calibrating of Eq. (15) gives the following results: $h_s = 4731$ MPa and $n = 0.1$.

According to Herle and Gudehus (1999), the value of parameter n can be calculated as follows:

$$n = \frac{\ln\left(\frac{e_{p1} C_{c2}}{e_{p2} C_{c1}}\right)}{\ln\left(\frac{p_1}{p_2}\right)}, \tag{19}$$

where e_{p_1} and e_{p_2} are void ratios corresponding to mean pressures p_1 and p_2 , respectively, and C_c coefficients are the corresponding compression indices (Fig. 4), defined as:

$$C_c = \frac{\Delta e}{\Delta \ln \left(\frac{p_s}{p_{s0}} \right)}. \quad (20)$$

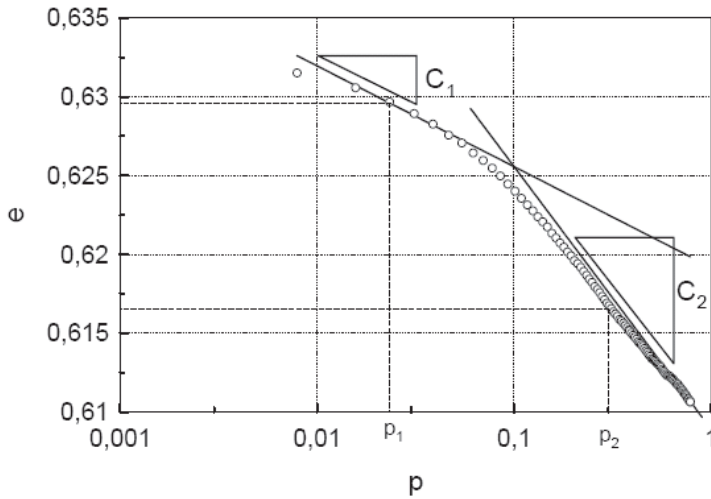


Fig. 4. Void ratio vs. mean stress during isotropic loading test

With already calculated n , h_s can be calculated as:

$$h_s = 3p \left(\frac{ne_p}{C_c} \right)^{\frac{1}{n}}. \quad (21)$$

Using this method, the following estimations have been obtained: $h_s = 1619$ MPa and $n = 0.359$.

3.4. α Parameter – Peak State Coefficient

This parameter informs about the extent to which the sand is compressed, when maximal vertical stress in triaxial compression test is reached. Parameter α appears in a very narrow range (~ 0.1 – 0.3) and is constant for material with similar granulometric properties. In the case of ‘Skarpa’ sand value 0.15 was taken as the first approximation. Full procedure of parameter α estimation was presented by Herle and Gudehus (1999) and will not be presented here.

3.5. β Parameter

This parameter does not practically depend on granulometric properties of sand, and for the majority of natural sands $\beta \simeq 1$ (see Appendix 1), it affects the shape of equation only, when void ratio e is significantly smaller than e_i , which occurs in the case of strongly compressed soil. β can be delivered from Eq. (6) with the assumption, that in the case of isotropic loading ($T_1 = T_2$) sand is isotropically compressed ($D_1 = D_2$).

For ‘Skarpa’ sand the value of β calculated this way is 1.02.

3.6. Minimalisation Procedure

For the purposes of this research the computer program was written. The first main function of this is to precisely determine parameters of von Wolffersdorff’s model using Powell’s non-gradient minimalisation procedure (Baron 1994, Press et al 1986), basing on previously estimated parameters, which are treated as initial values. The program uses files containing results of the experiment carried out on any straight path in the stress space. The second function of the program is to model the experiment performed in triaxial apparatus or in oedometer using delivered parameters. The author tried to use a number of programs written for these purposes, which were available on the Internet, but none of them was neither able to execute these tasks, nor enough user-friendly to use it.

The triaxial compression test data on dense ‘Skarpa’ sand (Fig. 5) were chosen to calibrate the equation (6). The set of parameters received was presented in Table 2.

Table 2. Parameters of von Wolffersdorff model for ‘Skarpa’ sand

	Triaxial compression test
φ_c	31°
h_s	5000 MPa
n	0.3
e_{d0}	0.432
e_{c0}	0.677
e_{i0}	0.8
α	0.26
β	0.97

Determined parameters of ‘Skarpa’ sand are comparable with those of ‘Hochstetten’ and ‘Schlabendorf’ sands, which have similar granulometric properties (Appendix 1).

Figures 6 and 7 show, how modelled sand should behave during triaxial compression test under various lateral pressures and initial void ratios (compare with Bauer 1996, Fig. 18).

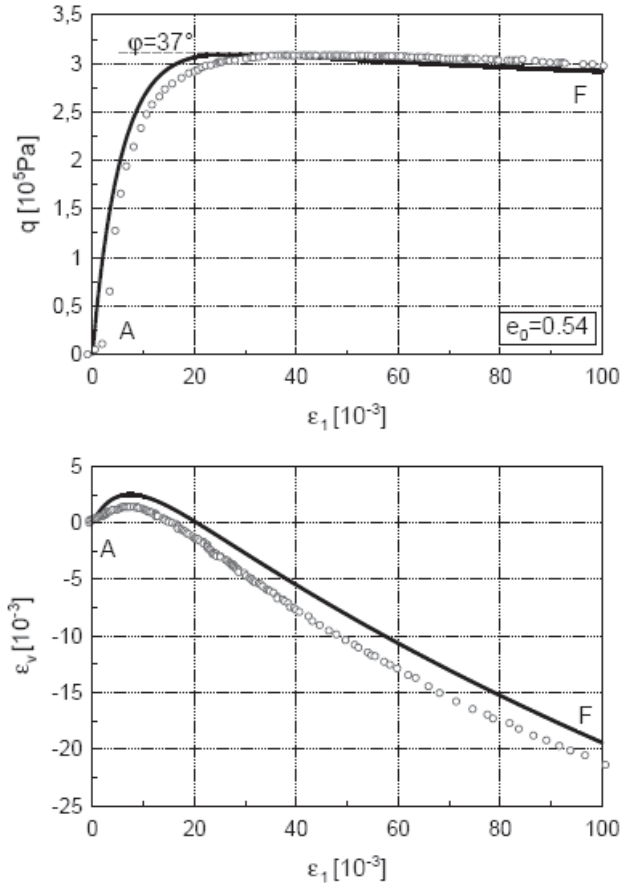


Fig. 5. Model calibrated to triaxial compression test for dense ‘Skarpa’ sand (letters A and F refer to Fig. 8); φ is the mobilized internal friction angle at peak

4. Verification of the Model

Verification of the model was carried out over many different cases. Theoretical predictions were compared with experiments conducted in the triaxial apparatus, as well as in the oedometer equipped with additional sensors to measure lateral stress.

4.1. Triaxial Apparatus

A number of stress paths in the p and q invariants’ space has been presented in Fig. 8. The dashed line (AF) represents the stress path used in calibration of the von Wolffersdorff model. By transition to the (σ_1, σ_3) coordinates, one can note, that this is the triaxial compression path – vertical stress increases while the

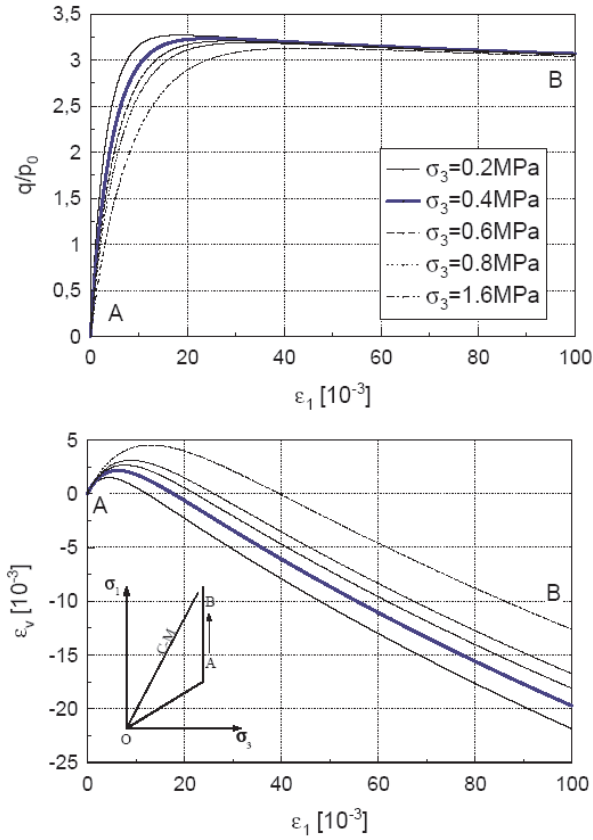


Fig. 6. Simulation of triaxial compression tests for various lateral pressures ($e_0 = 0.54$)

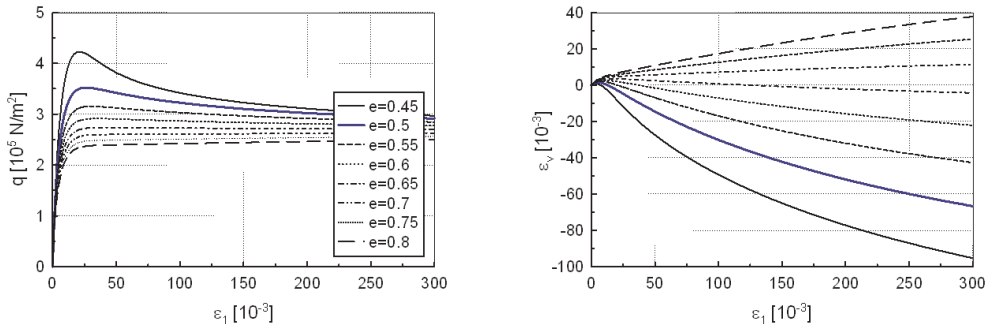


Fig. 7. Simulation of triaxial compression tests under various initial void ratios ($p_0 = 100 \text{ kPa}$)

lateral stress remains constant. Continuous lines represent the stress paths used for the verification of the model.

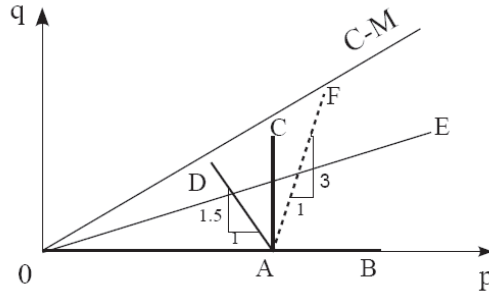


Fig. 8. The exemplary stress paths, that can be realized in the triaxial apparatus

4.1.1. Isotropic Loading and Unloading

Isotropic loading test is presented in Fig. 8 as 0B path. This test provides the information on whether the reaction of the soil is isotropic or anisotropic. The results of the experiments indicate, that reaction of ‘Skarpa’ sand is highly anisotropic and during the test also deviatoric strains develop. However, according to the model of von Wolffersdorff, in this case $\epsilon_q \approx 0$.

Predictions of volumetric strain, conducted for void ratios $e_0 = 0.63$ (loose) and $e_0 = 0.5$ (dense), are presented in Fig. 9. It could be seen, that calculated $\epsilon_v(p)$ corresponds to the experiments very well in the range of $p = 0$ to 0.8 MPa.

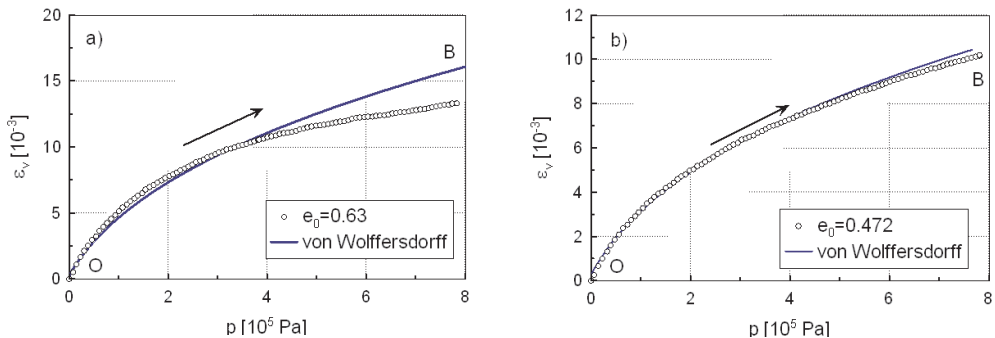


Fig. 9. Volumetric strain for a) loose, b) dense ‘Skarpa’ sand subjected to isotropic loading test. Solid line – von Wolffersdorff model; dotted line – experiment

After the loading test, the samples were unloaded to the initial state. Fig. 10 shows, how volumetric strain was developing during this phase. Experimental

curves on this figure were vertically shifted, to the ‘zero’ point. In this case a satisfactory prediction was not obtained (especially for the loose sand).

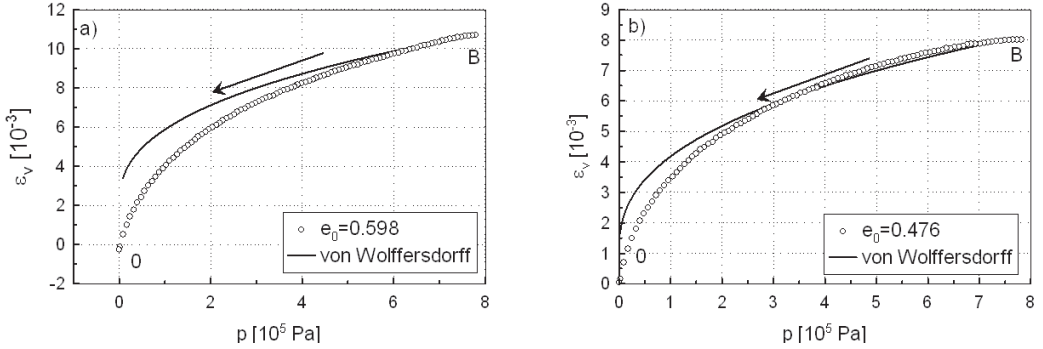


Fig. 10. Volumetric strain for a) loose, b) dense ‘Skarpa’ sand subjected to isotropic unloading. Solid line – von Wolffersdorff model; dotted line – experiment

Not too satisfactory prediction of deviatoric strains indicates that some modification of the model is required. Let us introduce the following relation:

$$F^2 D_1 \rightarrow F^2 D_1 + \gamma, \quad (22)$$

where $F^2 D_1$ is a linear component of equation (8), and γ is a parameter of anisotropy, determined experimentally. This modification was inspired by Niemunis (2003), who has implemented the inherent anisotropy to the stiffness, keeping the residual stress ratio unchanged. Results of modification (22) are presented in Fig. 11.

4.1.2. Deviatoric Loading and Unloading

Deviatoric loading and unloading is represented by ACA path in Fig. 8. First, sample is isotropically compressed (0A), then the stress deviator increases (AC) and decreases (CA), while mean stress is kept constant. During this particular experiment $p = 6$. Calculations were conducted for $e_0 = 0.64$ in case of loose sand (Fig. 12) and $e_0 = 0.49$ for dense sand (Fig. 13). Note that in this case the level of deformation is very small and does not exceed 1% of axial strain, as our goal is to study the pre-failure range of deformations.

Theoretical predictions of deformations of loose and dense sand on AC path within the range of 30% of axial strain are presented in Fig. 14.

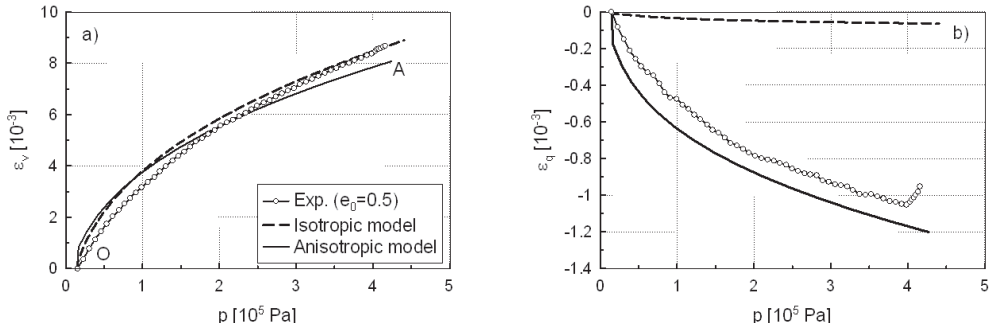


Fig. 11. a) volumetric and b) deviatoric strains for dense ($e_0 = 0.5$) ‘Skarpa’ sand subjected to isotropic loading. Dotted line – experiment, dashed line – von Wolffersdorff model, solid line – modified von Wolffersdorff model with $\gamma = 0.6$

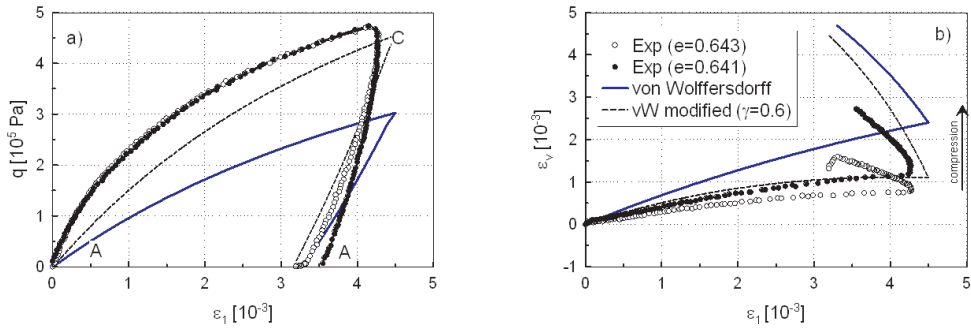


Fig. 12. a) stress deviator and b) volumetric strain for deviatoric loading and unloading of loose ‘Skarpa’ sand

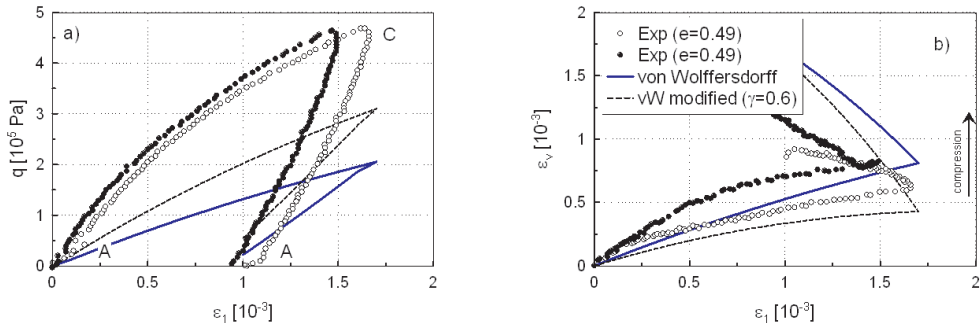


Fig. 13. a) stress deviator and b) volumetric strain for deviatoric loading and unloading of dense ‘Skarpa’ sand

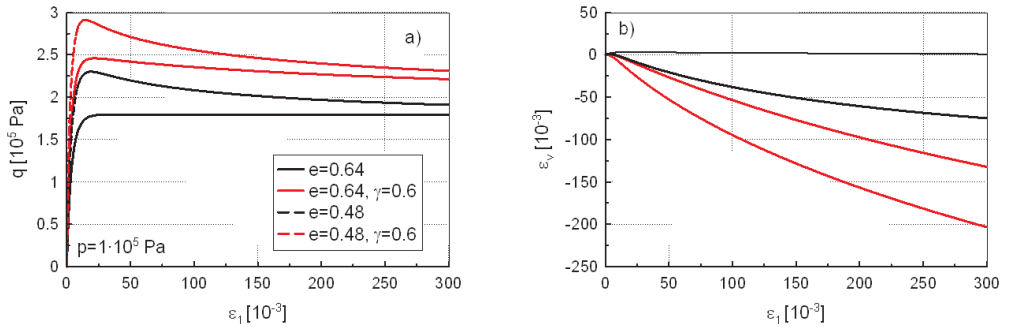


Fig. 14. Predictions of advanced deformations for AC path; a) stress deviator and b) volumetric strain vs. axial strain

4.2. Oedometer

Verification of the model was also carried out for loading and unloading in oedometric conditions. Calculated and measured data were plotted together in Fig. 15. 'Skarpa' sand sample used in this test was prepared with initial void ratio $e_0 = 0.55$.

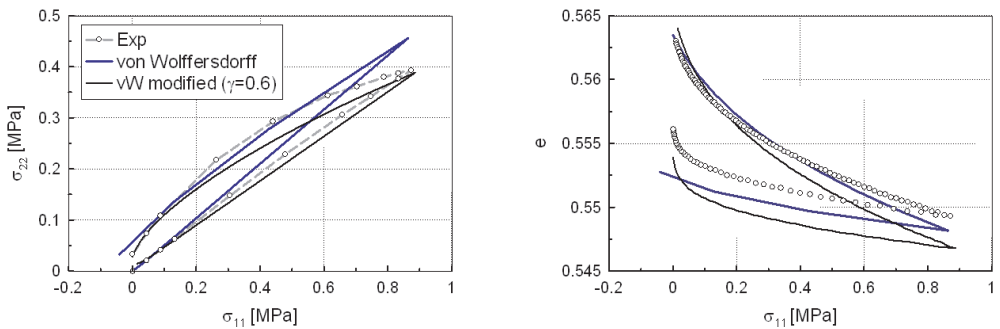


Fig. 15. Oedometer loading and unloading test

5. Summary

In the paper, modelling of deformations of sand subjected to different stress paths in triaxial conditions was presented. Deformations were calculated, using von Wolffersdorff's hypoplastic model. Two parameters were calibrated on the basis of the steady state line, while the remaining parameters were determined using classical methods. After that, parameters were precisely calibrated with the use of minimalisation procedure, where previously estimated parameters were

treated as initial values. The model can be calibrated based on the response of soil subjected to various stress paths in triaxial conditions and not only for standard triaxial compression test. Calibrated equation was verified for the triaxial as well as oedometric conditions.

Results indicate, that von Wolffersdorff's model predicts volumetric deformations with acceptable precision, but doesn't handle deviatoric strains. In order to resolve this problem, the modification of the model was proposed. This modification doesn't influence volumetric strains, but makes better prediction of deviatoric strains possible. It also improved predictions of deformations in the oedometer.

References

- Baron B. (1994), *Numerical Methods in Turbo Pascal*, Helion, Gliwice (in Polish).
- Bauer E. (1996), Calibration of a comprehensive hypoplastic model for granular materials, *Soils and Foundations*, Vol. 36, No. 1, 13–26.
- Gudehus G. (1996), A comprehensive constitutive equation for granular materials, *Soils and Foundations*, Vol. 36, No. 1, 1–12.
- Herle I., Gudehus G. (1999), Determination of parameters of a hypoplastic constitutive model from properties of grain assemblies, *Mech. Cohes.-Frict. Mater.*, 4, 461–486.
- Kolymbas D. (1985), A generalized hypoplastic constitutive law, *Proceed. 11th Int. Conf. Soil Mech. Found. Eng.*, Balkema 1988, Vol. 5, 2626.
- Matsuoka, H., Nakai T. (1977), Stress-strain relationship of soil based on the SMP, *Proceedings of Specialty Session 9, 9th International Conference on Soil Mechanics and Foundation Engineering (ICSMFE)*, 153–162.
- Niemunis A. (2003), Anisotropic effects in hypoplasticity, *3rd International Symposium on Deformation Characteristics of Geomaterials*, (Ed. Di Benedetto et al), 22nd–24th September 2003, Lyon, France, Vol. 1, 1211–1217.
- Press W. H., Teukolsky S. A., Vetterling W. T., Flannery B. P. (1986), *Numerical Recipes in FORTRAN 77, The Art of Scientific Computing*, Cambridge University Press.
- Sawicki A., Chybicki W. (2003), Modelling deformations of granular media before failure, *Inżynieria Morska i Geotechnika*, 24, 3–4, 190–194 (in Polish).
- Sawicki A., Świdziński W. (1995), Oedometric method of determination of elastic moduli for non-cohesive soils, *XLI Konferencja Naukowa Komitetu Inżynierii Lądowej i Wodnej PAN i Komitetu Nauki PZiTb*, 126–132 (in Polish).
- Sawicki A. (2003), Cam-clay approach to modelling pre-failure behaviour of sand against experimental data, *Archives of Hydro-Engineering and Environmental Mechanics*, Vol. 50, No. 3, 229–249.
- Świdziński W., Mierczyński J. (2002), On the measurement of strains in the triaxial test, *Archives of Hydro-Engineering and Environmental Mechanics*, Vol. 49, No. 1, 23–41.
- Świdziński W., Mierczyński J. (2005), Instability line as a basic characteristic of non-cohesive soils, *Archives of Hydro-Engineering and Environmental Mechanics*, Vol. 52, No. 1, 59–85.
- Tejchman J. (2004), Influence of a characteristic length on shear zone formation in hypoplasticity with different enhancements, *Computers and Geotechnics*, 31, No. 8, 595–611.
- Wolffersdorff P. A. von (1996), A hypoplastic relation for granular materials with a predefined limit state surface, *Mechanics of Cohesive-Frictional Materials*, 1, 251–271.

Appendix 1. List of von Wolffersdorff's parameters determined for some granular materials

Material	φ [°]	h_s [MPa]	n	e_{d0}	e_{c0}	e_{i0}	α	β
Toyoura sand	30	2600	0.27	0.61	0.98	1.10	0.18	1.00
Hochstetten sand	33	1500	0.28	0.55	0.95	1.05	0.25	1.50
Schlabendorf sand	33	1600	0.19	0.44	0.85	1.00	0.25	1.00
Hostun sand	31	1000	0.29	0.61	0.91	1.09	0.13	2.00
Karlsruhe sand	30	5800	0.28	0.53	0.84	1.00	0.13	1.05
Zbraslav sand	31	5700	0.25	0.52	0.82	0.95	0.23	1.00
Ottawa sand	30	4900	0.29	0.49	0.76	0.88	0.10	1.00
Ticino sand	31	5800	0.31	0.60	0.93	1.05	0.20	1.00
SLB sand	30	8900	0.33	0.49	0.79	0.90	0.14	1.00
Hochstetten gravel	36	32000	0.18	0.26	0.45	0.50	0.10	1.80
plastics	32	110	0.33	0.53	0.73	0.80	0.08	1.00
wheat	39	20	0.37	0.57	0.84	0.95	0.02	1.00
Skarpa sand	31	5000	0.3	0.43	0.68	0.8	0.26	0.97